

## Supplementary Videos

**Video 1.** A rotatable static packing of colloids in a cylindrical (ID = 0.1 mm) borosilicate capillary is imaged by ACT, demonstrating the same region of the sample from a wide and continuous range of angles. The particle radius is 2.5 – 3  $\mu\text{m}$  and the slices are taken at a depth of 20  $\mu\text{m}$  from the capillary wall. The total angle of sample rotation is  $30^\circ$ , well below the limitation of our setup (see Fig. S2).

**Video 2.** A non-rotatable static packing of colloids in a cylindrical (ID = 0.1 mm) borosilicate capillary is imaged by rotating the optical axis, employing an objective inverter (Fig. 1(b)). The particle radius is 2.5 – 3  $\mu\text{m}$ . Dark regions between the particles were formed by partial removal of the suspending liquid. These regions assist the eye in following the sample rotation. The slices are taken at a depth of 20  $\mu\text{m}$  from the capillary wall. The total angle of sample rotation is  $26^\circ$ , limited by the range of our vertical translation stage. With this limit removed, our setup allows the ACT data to be collected over a range of  $>200^\circ$ .

**Video 3.** The motion of colloidal particles within a ACT  $yz$ -slice [see Fig. 1(c)] is demonstrated by time series, with the refractive index of the capillary walls mismatching that of the objective immersion fluid [as in Fig. 3(a)]. Artificial dense fluctuating  $z$ -oriented particle chains are clearly visible in this concentrated suspension of PMMA particles. The solvent is an apolar density- and index- matching mixture of decahydronaphthalene and tetrachloroethylene. The movie is sped up for clarity.

**Video 4.** The same as in Video 3, but for a much lower particle concentration.

**Video 5.** A confocal volume scan of a binary mixture of small and large PMMA particles in an apolar (TCE:DHN) solvent. The scanning is done along the  $x$ -axis of the rectangular (0.1 $\times$ 2 $\times$ 50 mm) capillary (see the geometry in Fig. 1(c)). The Nikon type A oil is used for the objective immersion. While many chains are clearly visible, all of these apparent chains consist entirely of either the small or the large particles; no mixed chains occur. This observation confirms that these chains form due to an optical artifact, which gives rise to particle image multiplication along the  $z$ -axis of the capillary. Since density-matching of small and large particles in the same solvent is challenging, the sample was imaged a very short time after its shaking in a sonicator, so that a significant particle drift takes place. To increase the visibility of the smallest particles, the intensity of the large particles was increased to saturation. Note, every chain of particles shortens and converges into a single particle image when defocused; this shortening of defocused chains is an easily detectable fingerprint of the discussed optical artifact, allowing the artificial chains to be distinguished from the real ones, forming in other colloidal systems.

## Supplementary Figures

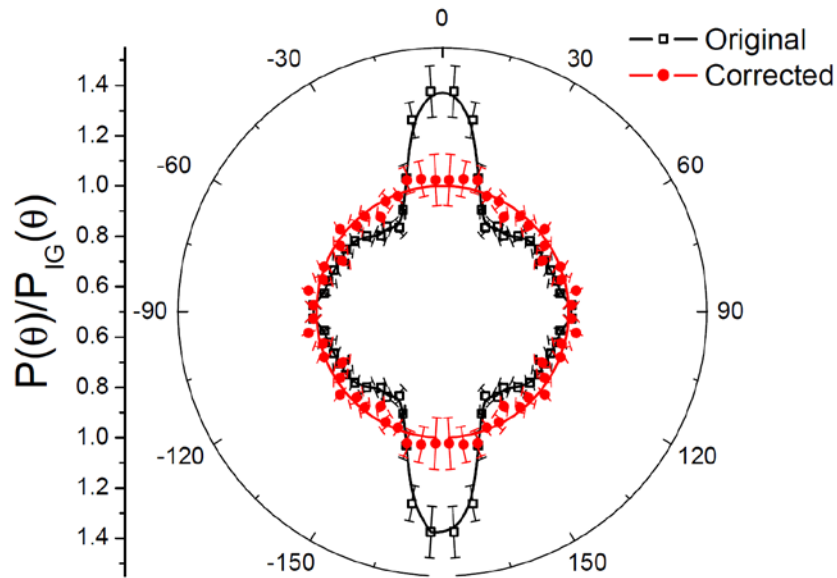


**Figure S1:** Inaccuracies in particle linking algorithms widely used for 3D confocal reconstructions of colloidal systems, give rise to apparent anisotropy in angular nearest neighbor distribution  $P(\theta, \phi)$  around the particle in a simple fluid (black symbols). As  $P(\theta, \phi)$  exhibits no dependence[1] on the azimuthal angle  $\phi$ , only the dependence on the polar angle  $\theta$  is shown here. To eliminate any possible effect of the illuminated volume boundaries on  $P(\theta, \phi)$ , the distribution is normalized by that of a simulated ideal gas  $P_{IG}(\theta, \phi)$ , filling an identical volume at the same particle number density. The  $P(\theta, \phi)$  peaks strongly along the optical axis of the system, suggesting z-oriented particle chains to be formed, breaking the rotational symmetry of the fluid. Depending on the linking parameters,  $P(\theta, \phi)$  may also be peaking at  $\theta = \pm 90^\circ$ . Following our ACT measurements, we could correct the particle linking algorithm (see main text), so that the resulting  $P(\theta, \phi)$  is perfectly isotropic (red symbols). The black curve is guide to the eye. The red curve corresponds to a perfectly isotropic distribution,  $P(\theta, \phi) = 1$ .

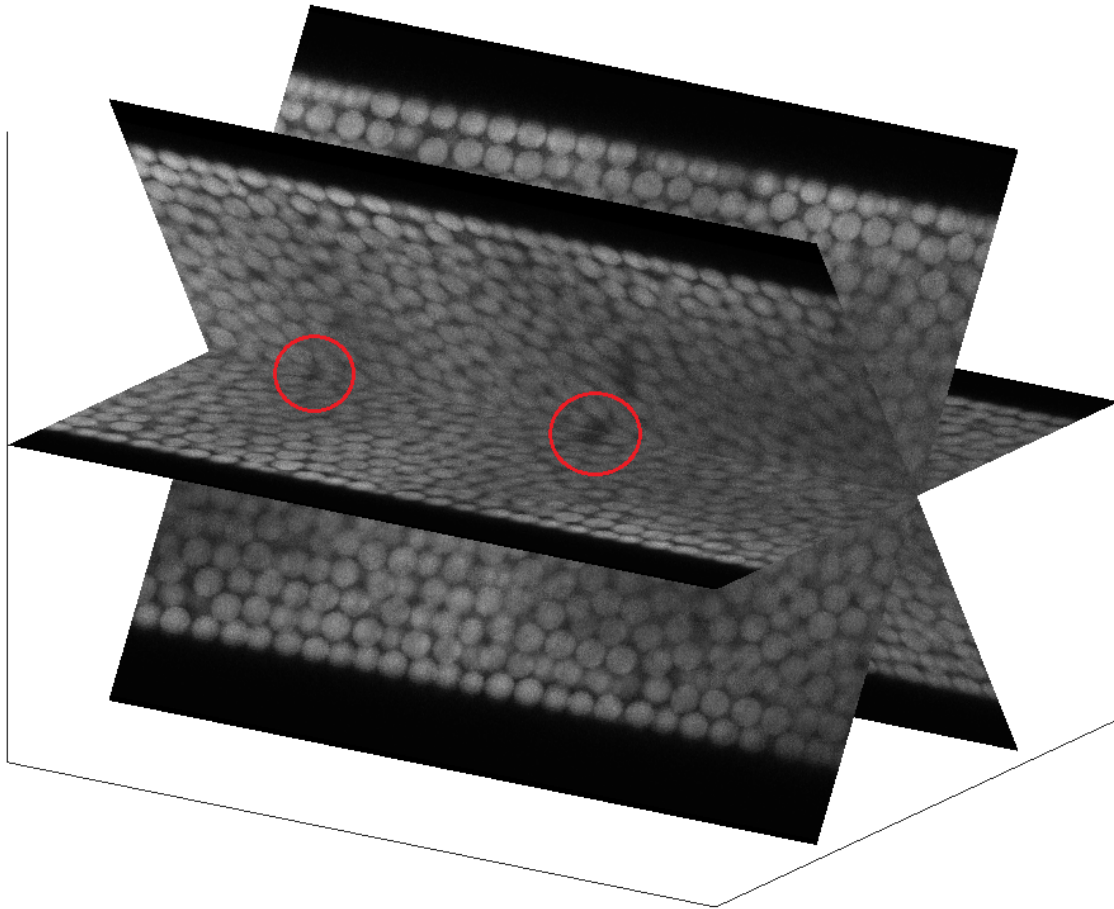


**Figure S2:** A collage of ACT cross sections taken through the same region of a dense colloidal sample. Two interparticle voids, clearly visible in two different cross sections, are encircled in red, demonstrating the very good mutual alignment of the cross sections. These cross sections slice through the center of a rotatable colloidal packing, contained in a cylindrical capillary. The walls of the capillary (ID = 0.1 mm) appear black at the edges of these confocal images. Particle radius is 2.5 - 3  $\mu\text{m}$ .

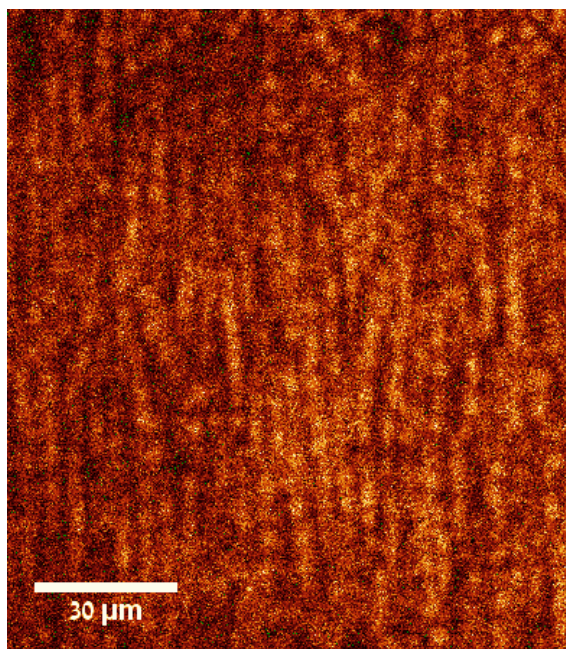


**Figure S3:** Artificial particle chains in 'side-view' ACT images of PMMA colloids, heat-shocked for rapid equilibration with the solvent (a density- and index- matching cis-decahydronaphthalene:tetrachloroethylene:tetrahydronaphthalene mixture). The fluorescent dye is covalently-linked to these colloids, allowing for the heat-shock procedure [2]. The colloids are contained in a 0.1×2×50 mm borosilicate Vitrocom<sup>TM</sup> capillary. The presence of artificial chains in this sample demonstrates that the phenomenon is insensitive to the particularities of colloidal synthesis.

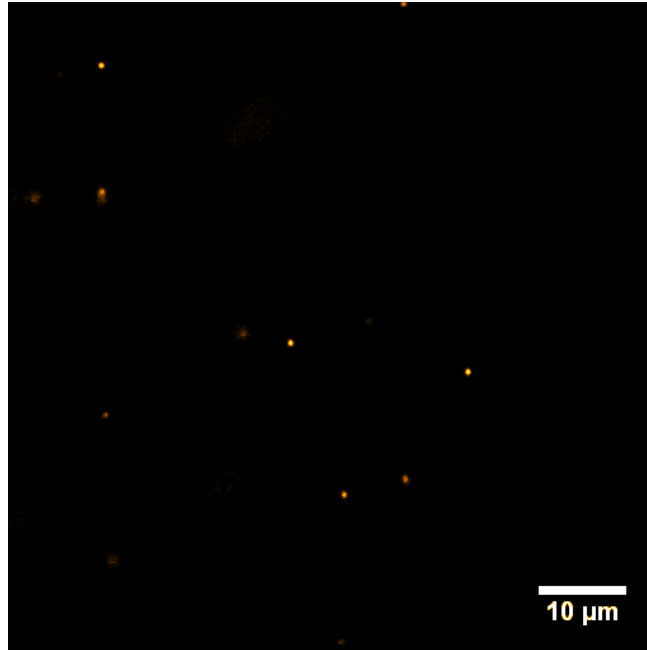


**Figure S4:** Silica particles with a fluorescein labelled fluorescent core[3] of diameter 200 nm and a total diameter of 850 nm, are suspended in glycerol ( $n=1.47$ ) and imaged through the curved side wall of the 0.2 x 2.0 x 50 mm Vitrocom<sup>TM</sup> borosilicate ( $n_{bs}=1.47$ ) capillary. Here, a glycerol-immersed 63X (NA=1.3) glycerol objective is used, with its correction collar set to a refractive index of  $n=1.47$ . Thus, the refractive indices of all the optical components are matched. Note the very sharp, no-aberration, images of the particles.

## References

- [1] Lu, P. J.; Shutman, M.; Sloutskin, E.; Butenko, A. V. Locating Particles Accurately in Microscope Images Requires Image-Processing Kernels to be Rotationally Symmetric. *Opt. Express* **2013**, *21*, 30755-30763.
- [2] Kodger, T. E.; Lu, P. J.; Wiseman, G. R.; Weitz, D. A. Stable, Fluorescent Polymethylmethacrylate Particles for the Long-Term Observation of Slow Colloidal Dynamics. *Langmuir* **2017**, *33*, 6382-6389.
- [3] van Blaaderen, A.; Vrij, A. Synthesis and Characterization of Colloidal Dispersions of Fluorescent, Monodisperse Silica Spheres. *Langmuir* **1992**, *8*, 2921-2931.